Peer-reviewed version available at Energies 2018, 11, 1931; doi:10.3390/en11081931

Article

ZnS/SiO_2 Passivation Layer for High-Performance of $TiO_2/CuInS_2$ Quantum Dot Sensitized Solar Cells

Hee-Je Kim [1], Jin-Ho Bae [1], Hyunwoong Seo [2], Masaharu Shiratani [2] and Chandu Venkata Veera Muralee Gopi [1,*]

[1] School of Electrical and Computer Engineering, Pusan National University, Busandaehak-ro 63beon-gil, Geumjeong-gu, Busan 46241, Korea; heeje@pusan.ac.kr (H.J.K.); bjhgood84@naver.com (J.H.B.);
[2] Department of Electronics, Kyushu University, 744 Motooka, Nishi-ku, Fukuoka, 819-0395, Japan; hw.seo@plasma.ed.kyushu-u.ac.jp (H.S.); siratani@ed.kyshu-u.ac.jp (M.S.);
* Correspondence: naga5673@gmail.com; Tel.: +8210-4940-0437

Abstract: Suppressing the charge recombination at the interface of photoanode/electrolyte is the crucial way to enhance the photovoltaic performance of quantum dot sensitized solar cells (QDSSCs). In this scenario, ZnS/SiO_2 blocking layer was deposited on $TiO_2/CuInS_2$ QDs to inhibit the charge recombination at photoanode/electrolyte interface. As a result, the $TiO_2/CuInS_2/ZnS/SiO_2$ based QDSSCs delivers a power conversion efficiency (η) value of 4.63%, which is significantly higher than the 2.15% and 3.23% observed for QDSSCs with a $TiO_2/CuInS_2$ device and $TiO_2/CuInS_2/ZnS$, respectively. Electrochemical impedance spectroscopy and open circuit voltage decay analyses indicate that ZnS/SiO_2 passivation layer on $TiO_2/CuInS_2$ suppress the charge recombination at the photoanode/electrolyte interface and prolongs the electron lifetime.

Keywords: QDSSCs; Charge recombination; ZnS/SiO_2; Passivation layer;

1. Introduction

Semiconductor quantum dots (QDs) based on II-VI group such as CdSe,[1] CdTe,[2] CdS,[3] PbS,[4] PbSe,[5] and etc. have been extensively studied for quantum dot sensitized solar cell (QDSSC) and photocatalysis applications, due to tunable band gap, high extinction coefficient, large intrinsic dipolar moment and multiple excition generation (MEG).[6,7] However, highly toxic Cd or Pb-containing QDs based solar cells show the excellent photostability and high power conversion efficiencies (PCEs), but the intrinsic high toxicity of Cd or Pd still limit the commercial applications in consideration of environmental and health concerns. Therefore, the development high quality "green" QDs sensitizers without carcinogenic heavy metal element is critical for the practical applications of QD based solar cells.

As an alternatives to the highly toxic Cd and Pb chalcogenide QDs, less-toxic I–III–VI_2 group QDs, especially $CuInS_2$ (CIS) QD has been attracted due to high absorption coefficient (~10^5 cm^{-1}) and near optimal band gap energy (1.0–1.5 eV), both of which make it a promising candidate as a sensitizer in QDSSCs [8-10]. There are two common approaches have been demonstrated for assembling $CuInS_2$ QDs onto TiO_2 electrodes: The first method uses presynthesized QDs onto TiO_2 surfaces through direct adsorption or bifunctional-linker-assisted adsorption and (2) the in situ preparation of QDs onto TiO_2 by successive ionic layer adsorption and reaction (SILAR) providing high surface coverage of QDs [11,12]. Owing to its facile and reproducible preparation, The SILAR process has recently emerged as the best method for adsorbing QDs onto TiO_2 electrodes with high

QD loading and well controllable in size and density of the target semiconductor QDs and efficient electron transfer to TiO_2 [13,14].

Chang *et al.* reported that $CuInS_2$ QD-sensitized TiO_2 nanoparticle film with a buffer layer (Cu_2S) and a passivation layer (ZnSe), fabricated by using the successive ionic-layer adsorption and reaction (SILAR) process and achieved a PCE of 2.52% [15]. Zhou *et al.* reported QDSSCs based on $CuInS_2$ and introduction of In_2S_3 buffer layer suing SILAR process, which presented as high as ~1.06% PCEs [16]. However, the lower photovoltaic performance of QDSSC is due to severe charge recombination process at the interface of the TiO_2/QD/electrolyte interface. To suppress charge recombination in sensitized cells, over coating the mesoporous oxide electrode with a thin wide band gap inorganic barrier layer, which act as an energy barrier preventing electrons from recombining. Until now, ZnS is the most popular photoanode coating material for preventing interfacial recombination in QDSSCs [17]. The ZnS over layer is introduced by the facile SILAR process, which covers the bare mesoporous TiO_2 alongside the surface of QDs toward the electrolyte. The ZnS coating was found to enhance the performance of solar cells due to the passivation of the QD surface states, resulting in suppression of the recombination processes within the cell. Interestingly, the combination of ZnS coating with different dipolar molecules absorbed on the TiO_2 surface has been demonstrated to improve the performance of QDSSCs [18].

Herein, we report that a novel ZnS/SiO_2 double barrier coating treatment, sequentially deposited after $CuInS_2$ QD on photoanode, attenuates substantially the recombination in QDSSCs. SiO_2 layer presents a high porosity with high micropore volume, which allows a good photogenerated hole capture by electrolyte from QD when it covers ZnS (ZnS/SiO_2). As a result the ZnS/SiO_2 on $CuInS_2$ favors the enhancement of photocurrent, photovoltage, and consequently the PCE of the resultant cell devices. The QDSSC based on the $CuInS_2$ QD sensitizer and ZnS/SiO_2 double layer exhibits a PCE of 4.63% (with short circuit current density (J_{SC}) = 12.83 mA cm^{-2}, an open circuit voltage (V_{OC}) = 0.603 V, fill factor (FF) = 0.598) under AM 1.5 G one full sun illumination, which is much higher than the $CuInS_2$/ZnS (PCE = 3.23%) and $CuInS_2$ (PCE = 2.15 %). Electrochemical impedance spectroscopy (EIS) and open circuit voltage decay (OCVD) measurements show that this ZnS/SiO_2 double layer significantly reduces the electron recombination at the photoanode/electrolyte interfaces.

2. Results and Discussion

2.1. Morphological characterization

Figure 1a, 1b, and 1c show the SEM images of the bare $CuInS_2$, $CuInS_2$/ZnS, and $CuInS_2$/ZnS/SiO_2 layers on the surface of TiO_2. The bare $CUInS_2$ film in Figure 1b exhibits uniformly distributed nanoparticles on the TiO_2 surface. The surface morphology of the samples were similar although there is a slight increase in the particle size of with the ZnS and ZnS/SiO_2 layer deposition; however, the exact change in size of particles is difficult to investigate and was inconclusive. Therefore, EDX and XPS measurements were conducted to identify the ZnS and ZnS/SiO_2 coatings on the surface of TiO_2. Moreover, the compositional distributions of a TiO_2/$CuInS_2$/ZnS/SiO_2 sample are further demonstrated by elemental mapping behavior, in which the homogeneous distribution and coexistence of Cu, In, Zn, S, Si and O elements are clearly observed in TiO_2/$CuInS_2$/ZnS/SiO_2 sample.

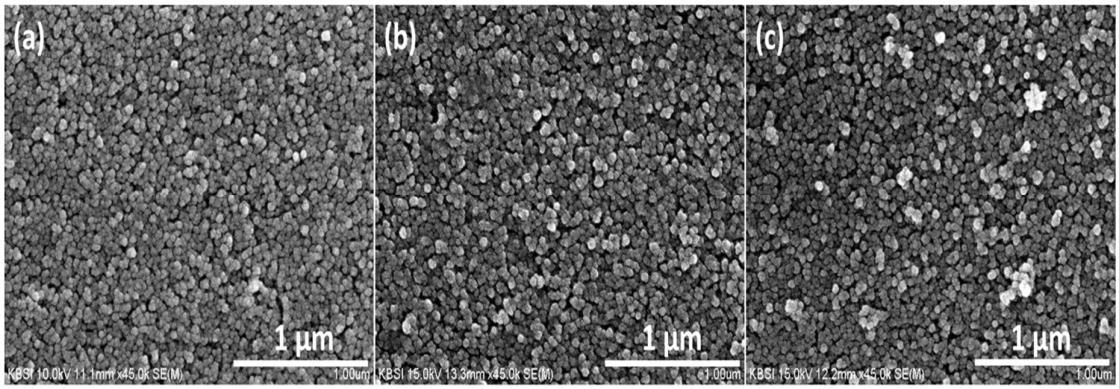

Figure 1 Surface SEM images of the (a) $CuInS_2$, (b) $CuInS_2/ZnS$, and (c) $CuInS_2/ZnS/SiO_2$ layers on the surface of TiO_2.

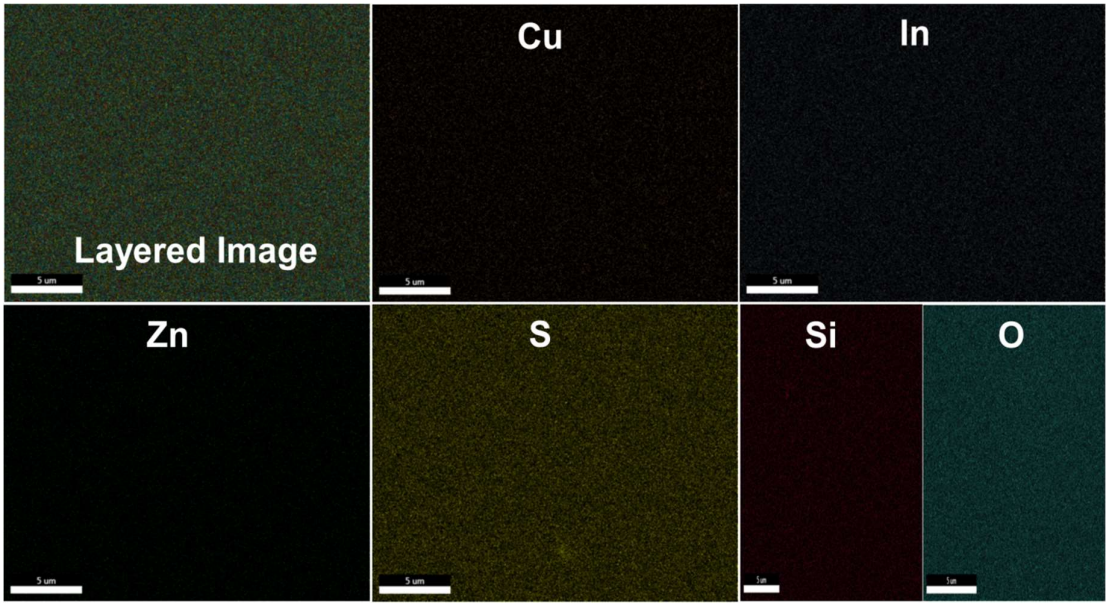

Figure 2 Elemental mapping images of the Cu, In, Zn, S, Si and O for the $TiO_2/CuInS_2/ZnS/SiO_2$ samples.

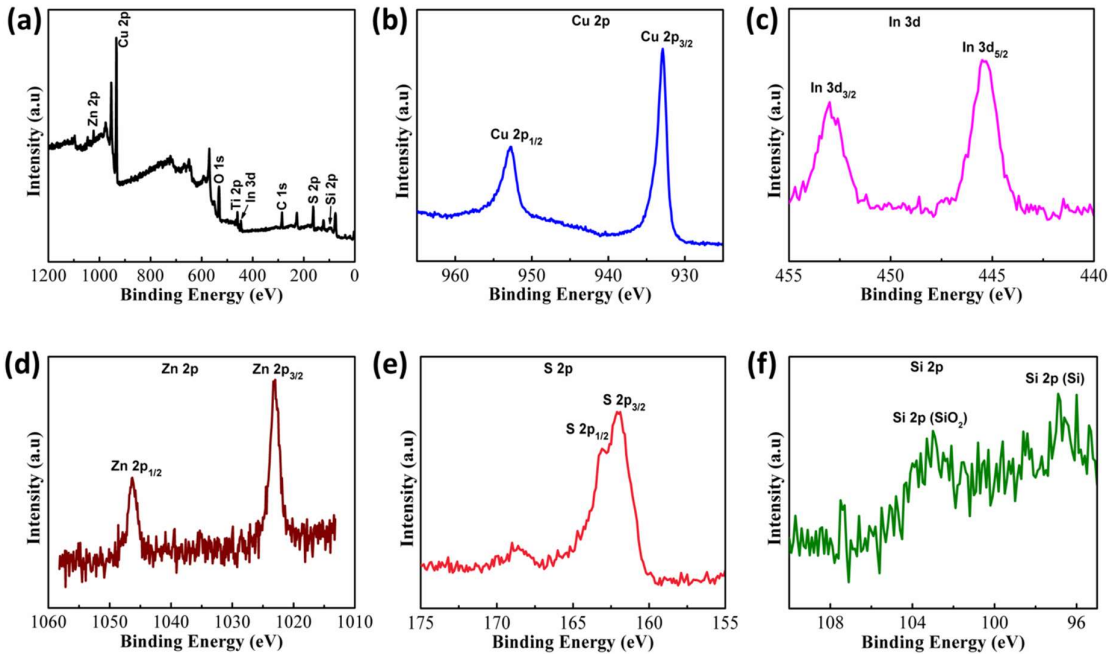

Figure 3 (a) XPS survey of $CuInS_2$ QDs adsorbed on the TiO_2 film. XPS spectrum of close-up survey in the (b) Cu 2p region, (c) In 3d region, (d) Zn 2p region, (e) S 2p region, and (d) Si 2p region.

The composition of the $CuInS_2/ZnS/SiO_2$ sample was investigated by XPS, as shown in Figure 3. The XPS survey spectra in Figure 3a depict peaks for Ti_{2p}, O_{1s}, C_{1s}, Cu_{2p}, In_{3d}, Zn_{2p}, S_{2p}, and Si_{2p}, respectively. The binding energy of Cu $2p_{3/2}$ and Cu $2p_{1/2}$ were observed at 932.9 and 952.7 eV, respectively (Figure 3b), with no evident shake-up satellite signals in this Cu2p spectrum. The two main peaks of In are located at 445.4 eV and 452.9 eV for In $3d_{5/2}$ and In $3d_{3/2}$, respectively (Figure 3c). Figure 3d depicts the binding energies for Zn $2p_{3/2}$ and Zn $2p_{1/2}$ of the prepared sample of $CuInS_2/ZnS/SiO_2$ at 1023.2 eV and 1046.2 eV respectively. The spectrum for S 2p was yielded peaks of S $2p_{3/2}$ and S $2p_{1/2}$ at binding energies of 162.0 eV and 163.0 eV, respectively (Figure 3e). The Si 2p spectrum (Figure 3f) exhibits a main peak and shoulder at lower binding energies. The main peak observed at 103.2 eV has been ascribed to Si in the oxidized form (SiO_2) and the other shoulder peak can be ascribed to the presence of crystalline Si (elemental Si).

2.2. Electrochemical characterization

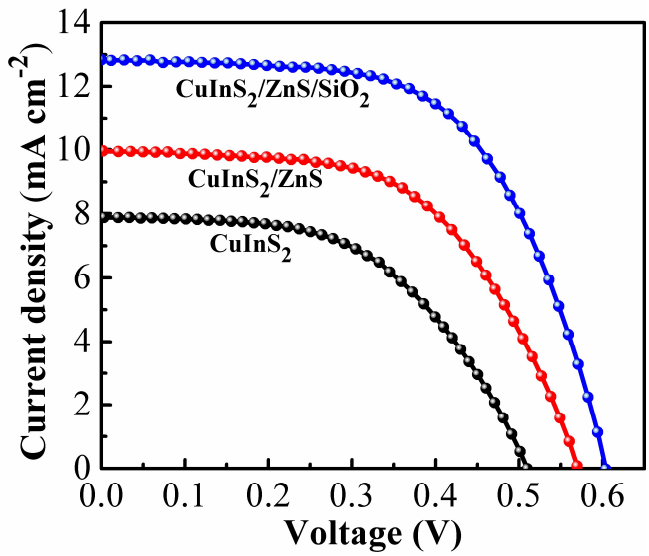

Figure 4 Current density-voltage (J-V) characteristics of $CuInS_2$, $CuInS_2$/ZnS and $CuInS_2$/ZnS/SiO_2 QDSSCs measured under the illumination of one sun (AM 1.5, 100 mW cm^{-2}).

The current density-voltage (J-V) curves of the QDSSCs based on various photoanodes were measured under AM 1.5 illumination (100 mW cm^{-2}) are shown in Figure 4 and the corresponding photovoltaic parameters are tabulated in Table 1. When only $CuInS_2$ are deposited on TiO_2 film, the QDSSC exhibits a J_{SC} of 7.87 mA cm^{-2}, V_{OC} of 0.509 V, FF of 0.537, resulting a low PCE of 2.15%. However, when ZnS and ZnS/SiO_2 passivation layers were deposited, all the photovoltaic parameters were greatly improved; the QDSSCs with a ZnS/SiO_2 layer exhibit the good performance, with J_{SC}, V_{OC}, and FF reaching 12.83 mA cm^{-2}, 0.603 V, and 0.598, respectively and the highest PCE of 4.63%, which is much higher than the PCE of 3.23% with a ZnS passivation layer. It is observed that the performance of QDSSC with a double layer of ZnS/SiO_2 is higher than that of ZnS passivation layer, which is due to suppression of recombination losses in QDSSCs and increases the charge collection efficiency.

Table 1 Summary of the photovoltaic properties and EIS results of QDSSCs fabricated various sensitized conditions

Cell	V_{oc} (V)	J_{sc} (mA cm^{-2})	FF	η%	R_S (Ω)	R_{CE} (Ω)	R_{ct} (Ω)
$CuInS_2$	0.509	7.87	0.537	2.15	9.34	0.84	30.65
$CuInS_2$/ZnS	0.569	9.95	0.571	3.23	10.03	1.03	23.95
$CuInS_2$/ZnS/SiO_2	0.603	12.83	0.598	4.63	10.24	1.16	55.02

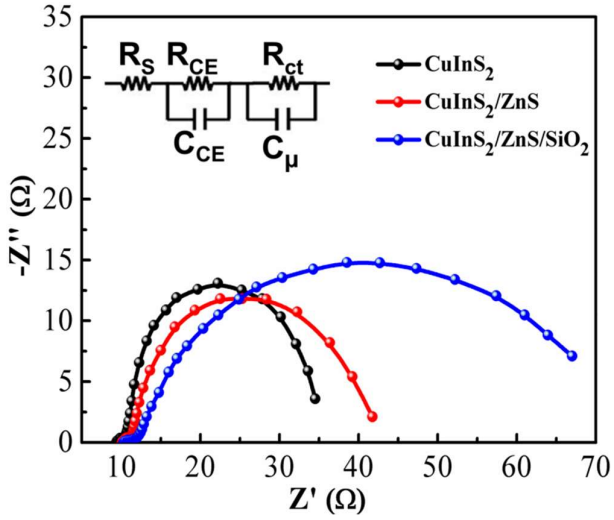

Figure 5 EIS curves of QDSSCs based $CuInS_2$ and $CuInS_2$/ZnS and $CuInS_2$/ZnS/SiO_2 cells in the form of Nyquist-plots and the inset shows the equivalent circuit used to fit the impedance spectra.

Electrochemical impedance spectroscopy (EIS) characterizations were conducted to investigate the charge recombination processes in devices under forward bias (V_{OC}) and dark condition. Figure 5 depicts the EIS spectra of $CuInS_2$ QDSSCs without and with ZnS or ZnS/SiO_2 passivation layers which were fitted using Z-view software with the equivalent circuit provided in the inset of Figure 5. The corresponding fitting results are shown in Table 1. The Nyquist plot consists of two semicircles and the first semicircle represents the resistance at the CE/electrolyte interface. The second semicircle represents the charge transfer resistance at the interface of the TiO_2/QDs/electrolyte. The intercept on the real axis of the impedance plot at higher frequency corresponds to the series resistance (R_s) of FTO substrate and the resistance of FTO/TiO_2 [19,20]. It is noticed that there are no apparent differences observed in the R_S and R_{CE} due to the same CE and electrolyte used in these experiments. However, there is a noticeable difference in R_{ct}; the R_{ct} value for the $CuInS_2$/ZnS/SiO_2 based QDSSCs is 55.02 Ω, while R_{ct} value for the $CuInS_2$/ZnS and $CuInS_2$ based QDSSCs are only 30.65 Ω and 23.95 Ω, respectively. The charge recombination resistance at the interface of TiO_2/QDs/electrolyte is mainly determined by R_{ct}. The higher R_{ct} value represents the reduced recombination of the electrons and holes, and enhances the electron transfer process at TiO_2/QDs/electrolyte interface. Therefore, it is confirmed that the deposition of ZnS/SiO_2 passivation layer on the $CuInS_2$ QDs favors the efficient electron transfer from $CuinS_2$ to TiO_2 photoanodes with suppression of the interfacial charge recombination processes, which is more effectively than that of the ZnS passivation layer.

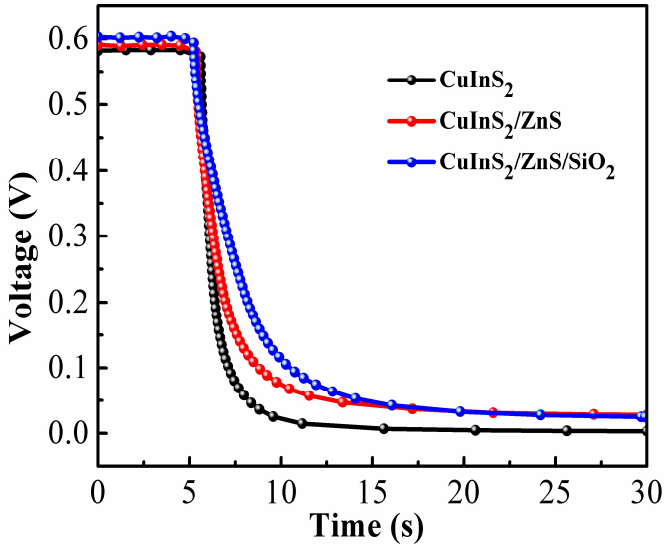

Figure 6 Open circuit decay curves of QDSSCs based $CuInS_2$ and $CuInS_2$/ZnS and $CuInS_2$/ZnS/SiO_2 cells.

Furthermore, open circuit voltage decay (OCVD) measurements were carried out to investigate the charge recombination process in QDSSCs and the results. OCVD analysis of QDSSCs was performed during relaxation form an illuminated quasiequilibrium state to the darkness. Figure 6 depicts the OCVD plots of the QDSSCs based on $CuInS_2$, $CuInS_2$/ZnS and $CuInS_2$/ZnS/SiO_2 photoanodes. Apparently, the $CuInS_2$/ZnS/SiO_2 cell delivered considerably longer decay times than the $CuInS_2$ and $CuInS_2$/ZnS cells, indicating a suppression of charge recombination process. Moreover, the V_{OC} decay is directly related to the electron life time according to following equation [21]:

$$\tau_e = -\left(\frac{k_B T}{e}\right)\left(\frac{dV_{OC}}{dt}\right)^{-1} \quad (1)$$

where k_B is the Boltzmann constant, T is the absolute temperature , and e is the electronic charge. Figure 5b depicts the electron life time (τ_e, in a log representation) as a function of V_{OC}. It can be noticed that the τ_e of all the devices increases with decreasing V_{OC}. Among the QDSSCs investigated, the $CuInS_2$/ZnS/SiO_2 delivers longer τ_e than the $CuInS_2$/ZnS and $CuInS_2$ devices, implying suppressed recombination and efficient electron transfer at the TiO_2/QDs/electrolyte, which is consistent with EIS analysis. Therefore, the slower V_{OC} decay and longer τ_e of the $CuInS_2$/ZnS/SiO_2 device efficiently suppressed the electron recombination from TiO_2 and QDs to electrolyte and higher charge collection efficiency contribute to the enhanced photovoltaic performance.

Peer-reviewed version available at Energies 2018, 11, 1931; doi:10.3390/en11081931

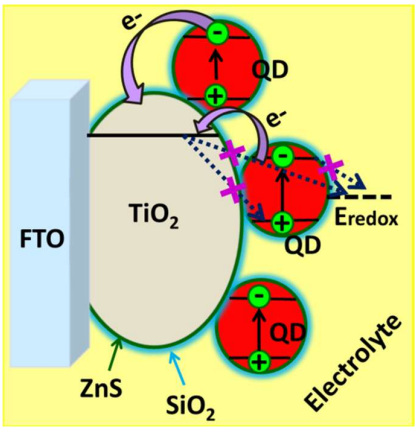

Figure 7 Schematic illustration of the possible charge transfer mechanism in the $TiO_2/CuInS_2/ZnS/SiO_2$ QDSSCs.

Several paths for charge recombination occurs in the QDSSCs, in which the excited electrons from the TiO_2 can react with the electrolyte or with the QDs and photo excited electrons from the QDs react with the electrolyte. The deposition of ZnS/SiO_2 layer on the surface of $TiO_2/CuInS_2$ can effectively suppress the charge recombination process at the photoanode/electrolyte interface (Figure 7) and improve the photovoltaic performance of QDSSCs.

4. Materials and Methods

4.1. Preparation of TiO_2 electrodes

TiO_2 film was fabricated by doctor blading the TiO_2 paste (20 nm, Ti-Nanoxide HT/TP, Solaronix) on well-cleaned fluorine-doped tin oxide (FTO, 1.3×1.6 cm^2) substrate with an active area of 0.25 cm^2. The film was then heated at 450 ^oC for 30 min and producing a thickness of 7.5 μm after solvent evaporation [22].

4.1. Deposition of $CuInS_2$ QDs on TiO_2 electrodes

$CuInS_2$ QDs was deposited on the TiO_2 substrate using the successive ion layer adsorption and reaction (SILAR) process. TiO_2 electrodes were successively immersed into the three different solutions: one of 0.05 M of $Cu(NO_3)_2$ for 2 min, another of 0.05 M of $In(NO_3)_3$ for 2 min, and a final one of 0.1 M of Na_2S for 5 min. Following each immersion, the films were rinsed with deionized (DI) water for 1 min to remove the excess precursors. This procedure comprises one $CuInS_2$ SILAR cycle and was repeated six times.

4.3. Deposition of ZnS, ZnS/SiO_2 passivation layers on $TiO_2/CuInS_2$ electrodes

The ZnS passivation layer was deposited on $TiO_2/CuInS_2$ electrodes by a SILAR process. Typically, $TiO_2/CuInS_2$ electrodes were successively immersed into aqueous solutions containing 0.1 M of $Zn(NO_3)_2$ and 0.1 M Na_2S for 1 min, respectively. This process was repeated for three times and the electrode is named as $CuInS_2/ZnS$. Furthermore, SiO_2 coating was carried out by dipping the

$CuInS_2$/ZnS electrodes in 0.01 M tetraethylorthosilicate ethanol solution containing 0.1 M NH_4OH for 1 h. The as-fabricated electrode is termed as $CuInS_2$/ZnS/SiO_2.

4.4. QDSSC fabrication

CuS counter electrode (CE) on FTO substrate was prepared according to the literature [23]. The photoanode was clamped with CuS CE using sealant ((SX 1170-60, Solaronix) at 100 °C) and the space between the electrodes was filled with polysulfide electrolyte (1 M Na_2S, 2 M S, and 0.2 M KCl in methanol and water at a ratio of 7:3).

4.5. Characterizations

The surface morphology and elemental composition of the electrodes were investigated using a scanning electron microscopy (SEM, S-2400, Hitachi) equipped with energy-dispersive X-ray spectroscopy (EDX) operated at 15 kV. The current-voltage (J-V) characteristics of the QDSSCs were examined under one sun illumination (AM 1.5G, 100 mW cm^{-2}) using an ABET Technologies (USA) solar simulator with an irradiance uniformity of ±3%. Electrochemical impedance spectroscopy (EIS) EIS was investigated using a BioLogic potentiostat/galvanostat/EIS analyzer (SP-150, France) under one sun illumination with a frequency of 100 mHz-500 kHz and 10 mV of AC amplitude.

5. Conclusions

Introduction of ZnS/SiO_2 passivation layer on TiO_2/$CuInS_2$ QDs has been demonstrated to be an efficient and promising approach to significantly suppress the charge recombination at photoanode/electrolyte and enhance the power conversion efficiency. Eventually, an overall η of 4.63% was obtained for the TiO_2/$CuInS_2$/ZnS/SiO_2 QDSSCs, which is approximately 43% enhancement over the η = 3.23% for the TiO_2/$CuInS_2$/ZnS QDSSCs and more than 115% increment over the η = 2.15% for the device without a passivation layer (TiO_2/$CuInS_2$). Overall, the method of a ZnS/SiO_2 passivation layer is an effective approach to enhance the overall power conversion efficiency of QDSSCs.

Acknowledgments: This research was supported by Basic Science Research Program through the National Research Foundation of Korea (NRF) funded by the Ministry of Education, ICT and Future planning (NRF-2016K2A9A2A08003717).

Author Contributions: The idea of this study was conceptualized by Hee Je Kim. Jin-Ho Bae, Hyunwoong Seo and Masaharu Shiratani helped to organize the data and prepare the research manuscript. Chandu Venkata Veera Muralee Gopi contributed to the conception and design of the experiment, analysis of the data, preparation of the devices, device performance measurements and writing the manuscript.

Conflicts of Interest: The authors declare no conflict of interest.

References

1. Lee, H.J.; Wang, M.; Chen, P.; Gamelin, D.R.; Zakeeruddin, S.M.; Grätzel, M.; Nazeeruddin, Md.K. Efficient CdSe Quantum Dot-Sensitized Solar Cells Prepared by an Improved Successive Ionic Layer Adsorption and Reaction Process. *Nano Lett.* 2009, *9*, 4221–4227.
2. Shen, X.; Jia, J.; Lin, Y.; Zhou, X. Enhanced performance of CdTe quantum dot sensitized solar cell via anion exchanges. *J. Power Sources* **2015**, *277*, 215-221.
3. Gopi, C.V.V.M.; Haritha, M.V.; Kim, S.K.; Kim, H.J. A strategy to improve the energy conversion efficiency and stability of quantum dot-sensitized solar cells using manganese-doped cadmium sulfide quantum dots. *Dalton Trans.* **2015**, *44*, 630–638.

4. Gonza´lez-Pedro, V.; Sima, C.; Marzari, G.; Boix, P.P.; Gime´nez, S.; Shen, Q.; Dittrich, T.; Sero, I.M. High performance PbS Quantum Dot Sensitized Solar Cells exceeding 4% efficiency: the role of metal precursors in the electron injection and charge separation. *Phys. Chem. Chem. Phys.* **2013**, *15*, 13835-13843.
5. Zhang, J.; Gao, J.; Church, C.P.; Miller, E.M.; Luther, J.M.; Klimov, V. I.; Beard, M.C. PbSe Quantum Dot Solar Cells with More than 6% Efficiency Fabricated in Ambient Atmosphere. *Nano Lett.* **2014**, *14*, 6010−6015.
6. Kamat, P.V. Quantum Dot Solar Cells. Semiconductor Nanocrystals as Light Harvesters. *J. Phys. Chem. C.* **2008**, *112*, 18737–18753.
7. Kongkanand, A.; Tvrdy, K.; Takechi, K.; Kuno, M.; Kamat, P.V.; Quantum Dot Solar Cells. Tuning Photoresponse through Size and Shape Control of CdSe−TiO_2 Architecture. *J. Am. Chem. Soc.* 2008, *130*, 4007–4015.
8. Booth, M.; Brown, A.P.; Evans, S.D.; Critchley, K. Determining the Concentration of $CuInS_2$ Quantum Dots from the Size-Dependent Molar Extinction Coefficient. *Chem. Mater.* **2012**, *24*, 2064−2070.
9. Leach, A.D.P.; Macdonald, J.E. Optoelectronic Properties of $CuInS_2$ Nanocrystals and Their Origin. *J. Phys. Chem. Lett*. **2016**, *7*, 572−583.
10. Li, T.L; Lee, Y.L.; Teng H. $CuInS_2$ quantum dots coated with CdS as high-performance sensitizers for TiO_2 electrodes in photoelectrochemical cells. *J. Mater. Chem.* **2011**, *21*, 5089–5098.
11. Bang, J.H.; and Kamat, P.V. Quantum Dot Sensitized Solar Cells. A Tale of Two Semiconductor Nanocrystals: CdSe and CdTe. *ACS Nano* **2009**, *3*, 1467–1476.
12. Lee, H.; Wang, M.K.; Chen, P.; Gamelin, D.R.; Zakeeruddin, S.M.; Gratzel, M.; Nazeeruddin, M.K. Efficient CdSe Quantum Dot-Sensitized Solar Cells Prepared by an Improved Successive Ionic Layer Adsorption and Reaction Process. *Nano Lett.* **2009**, *9*, 4221–4227.
13. Kontos, A.G.; Likodimos, V.; Vassalou, E.; Kapogianni, I.; Raptis, Y.S.; Raptis, C.; Falaras, P. Nanostructured titania films sensitized by quantum dot chalcogenides. *Nanoscale Res. Lett.* **2011**, *6*, 266–271
14. Lee, H.J.; Bang, J.; Park, J.; Kim S.; Park, S.M. Multilayered semiconductor (CdS/CdSe/ZnS)-sensitized TiO_2 mesoporous solar cells: all prepared by successive ionic layer adsorption and reaction processes. *Chem. Mater*. **2010**, *22*, 5636–5643.
15. Chang, J.Y.; Su, L.F.; Li, C.H.; Chang, C.C.; Lin, J.M. Efficient "green" quantum dot-sensitized solar cells based on Cu_2S–$CuInS_2$–ZnSe architecture. *Chem. Commun.* **2012**, *48*, 4848–4850.
16. Zhou, Z.; Yuan, S.; Fan, J.; Hou, Z.; Zhou, W.; Du, Z.; Wu, S. $CuInS_2$ quantum dot-sensitized TiO_2 nanorod array photoelectrodes: synthesis and performance optimization, *Nanoscale Res. Lett*. **2012**, *7*, 652.
17. Diguna, L.J.; Qing, S.; Kobayashi, J.; Toyoda, T. High efficiency of CdSe quantum-dot-sensitized TiO_2 inverse opal solar cells. *Appl. Phys. Lett.* **2007**, *91*, 023116.
18. de la Fuente, M.S.; Sanchez, R.S.; Gonza´ lez-Pedro, V.; Boix, P.P.; Mhaisalkar, S.G.; Rincon, M. E.; Bisquert, J.; Mora-Sero´, I.´ Effect of Organic and Inorganic Passivation in Quantum-Dot-Sensitized Solar Cells. *J. Phys. Chem. Lett.* **2013**, *4*, 1519−1525.
19. Gopi, C.V.V.M.; Haritha, M.V.; Kim, S.K.; Kim, H.J. Improved photovoltaic performance and stability of quantum dot sensitized solar cells using Mn–ZnSe shell structure with enhanced light absorption and recombination control. *Nanoscale* **2015**, *7*, 12552–12563.
20. Kim, H.J.; Kim, S.W.; Gopi, C.V.V.M.; Kim, S.K.; Rao, S.S.; Jeong, M.S. Improved performance of quantum dot-sensitized solar cells adopting a highly efficient cobalt sulfide/nickel sulfide composite thin film counter electrode. *J. Power Sources* **2014**, *268*, 163-170.

21. Liu, Z.; Miyauchi, M.; Uemura, Y.; Cui, Y.; Hara, K.; Zhao, Z.; Sunahara, K.; Furube, A. Enhancing the performance of quantum dots sensitized solar cell by SiO_2 surface coating. *Appl. Phys. Lett.* **2010**, *96*, 233107.
22. Kim, H.J.; Kim, D.J.; Rao, S.S.; Savariraj, A.D.; Kyoung, K.S.; Son, M.K.; Gopi, C.V.V.M.; Prabakar, K. Highly efficient solution processed nanorice structured NiS counterelectrode for quantum dot sensitized solar cell. *Electrochim. Acta* **2014**, *127*, 427–432.
23. Kim, H.J.; Sik, L.M.; Gopi, C.V.V.M.; Haritha, M.V.; Rao, S.S.; Kim, S.K. Cost-effective and morphology controllable PVP based highly efficient CuS counter electrodes for high-efficiency quantum dot-sensitized solar cells. *Dalton Trans.* **2015**, *44*, 11340-11351.